Biomaterials Science

RSC Publishing

PAPER

View Article Online
View Journal | View Issue

Micromechanical characterization of spider silk particles†

Cite this: *Biomater. Sci.*, 2013, **1**, 1160

Martin P. Neubauer,‡[a] Claudia Blüm,‡[b] Elisa Agostini,[c] Julia Engert,[c] Thomas Scheibel*[b] and Andreas Fery*[a]

Received 27th April 2013,
Accepted 28th June 2013

DOI: 10.1039/c3bm60108k

www.rsc.org/biomaterialsscience

Spider silk fibers are well known for their mechanical properties, and they are therefore in the focus of materials scientists. Additionally, silks display biocompatibility making them interesting materials for applications in medicine or cosmetics. Due to the low abundance of natural spider silk proteins because of the spider's cannibalism, the recombinant spider silk protein eADF4 has been established for material science applications. Once processed into micron-sized particles by controlled salting-out, these particles can be used as drug delivery vehicles. For any application of the silk particles it is important to know their mechanical characteristics for processing and storage reasons. Here, we examine the swelling behavior and mechanics of these particles. Upon hydration, a drastic drop in elastic modulus occurs by orders of magnitude, from 0.8 GPa in the dry state to 2.99 MPa in the wet state. Importantly, the elastic modulus of recombinant silk particles can be tuned by varying the molecular weight of the used proteins, as well as chemical crosslinking thereof.

Published on 25 July 2013.

Introduction

Spider silk has been in the focus of research for a long time, mainly due to its mechanical properties which are unique and which will be suitable for various applications. Unlike in nature, where spider silk proteins are typically processed into fibers, recombinant spider silk proteins can be processed into various other morphologies like particles, capsules, non-woven meshes or hydrogels.[1–6] It has previously been shown that the recombinant spider silk protein eADF4 can be processed into particles with controllable diameters by salting out.[1,2] Such silk particles consist of a solid core with high β-sheet content (around 60%) and a smooth surface.[2] Previously, eADF4(C16) particles were examined as possible drug delivery systems for medical and pharmaceutical applications.[1,7,8] Loading of particles with water soluble low molecular weight substances was achieved either by diffusion processes or by co-precipitation of the potential drug molecules together with the protein.[7] Additionally, incorporation of proteins into these particles has been shown by using lysozyme as a model substrate.[9] Substrate release could be achieved by diffusion,[7,8] and an accelerated release profile was gained by controlled enzymatic degradation of eADF4(C16).[10] The same publication demonstrated that the particles *e.g.* are selectively degraded in intestine fluids.

Within the past decade the atomic force microscope (AFM) has been established as the standard device to examine mechanical properties on the nano- and micro-scale.[11,12] In particular, a colloidal probe (CP) technique offers a valuable means of studying particle mechanics on a single particle level as well as surface interaction forces.[13–15] In biological investigations CP-AFM is even employed to analyze the stiffness and deformation behavior of entire cells.[16]

Here, we investigated the swelling behavior of dried eADF4(C16) particles upon hydration and their mechanical properties in the dry and wet state. Both are important regarding technical production processes and potential storage conditions, during which particles might undergo drying and rehydration steps. Applications in composite materials, *e.g.* bone substitute materials, will expose the particles to high mechanical stress, and therefore the mechanical properties have to be determined before employing spider silk particles as a filler of composites to reinforce materials. The surface properties of particles are also of high importance regarding future applications and have been analyzed separately.[17]

[a]*Physical Chemistry II, University of Bayreuth, Universitätsstr. 30, Bayreuth 95440, Germany. E-mail: Andreas.Fery@uni-bayreuth.de; Fax: +49 (0)92155 2059; Tel: +49 (0)921 55 2753*

[b]*Lehrstuhl Biomaterialien, University of Bayreuth, Bayreuth 95440, Germany. E-mail: Thomas.Scheibel@uni-bayreuth.de; Fax: +49 (0)92155 7346; Tel: +49 (0)921 55 7361*

[c]*Lehrstuhl für Pharmazeutische Technologie und Biopharmazie, LMU München, Butenandtstr. 5-13, München 81377, Germany*

†Electronic supplementary information (ESI) available. See DOI: 10.1039/c3bm60108k

‡Authors contributed equally to the work of the manuscript.

Results and discussion

Mechanical analysis and swelling behavior

First, the general deformation behavior of eADF4(C16) particles was analyzed by using a colloidal probe technique (Fig. 1 ESI a†), where the sharp tip of the AFM cantilever was replaced by a glass bead. For data evaluation we used a theoretical model based on the work of Hertz, which describes the elastic compression of two spheres in axially symmetric geometry.[18] Precise alignment is guaranteed by optical control. Our measurements revealed continuous deformation behavior without buckling features, indicating high homogeneity of the silk particles (Fig. 1 ESI b, c†).

Dry eADF4(C16) particles (Fig. 1a) are round shaped and have a smooth surface. They showed an average elastic modulus of 0.8 GPa ± 0.5 GPa, which compares well with previous experiments. Spiess *et al.* performed tensile tests on dried cast silk films (10–12 microns thick) yielding a Young's modulus between 2 and 4 GPa, depending on solvents and post-treatment.[19] From indentation measurements on 50 micron thick dry C16 films, Junghans *et al.* determined an elastic penetration modulus of 269 ± 91 MPa.[20]

Testing the fatigue behaviour in 51 cycles of deformation and relaxation, dry eADF4(C16) particles showed a shift in the contact point and a significant increase in elastic modulus with ongoing deformations (Fig. 1b and Fig. 2 ESI†). This plastic deformation behavior in combination with the high elastic modulus in the GPa range indicates a glassy state of the examined particles, which is confirmed by differential scanning calorimetry (DSC) and thermogravimetric analysis (TGA) (Fig. 1c and data not shown).

The thermal decomposition temperature is independent of the molecular weight of the silk protein at around 310 °C, close to the values previously detected for eADF4(C16) films.[19] The high elastic modulus and the remarkably high thermal decomposition temperature of dried silk particles could be used for distinct technical applications, *e.g.* as part of composite/particle reinforced materials.

Regarding the potential as drug delivery vehicles, the hydrated state of eADF4 particles was mechanically analyzed. Upon hydration, eADF4(C16) particles showed a significant and fully reversible increase in volume (Fig. 2a–d). During water adsorption, the volume of particles was more than doubled with a swelling factor of 2.31 ± 0.06. Swelling of the particles is considered to be a typical solvation effect as known from polymer theory.[21] Even after 10 cycles of water adsorption and desorption, the hydration behavior of the particles did not change (Fig. 2d). This enables the particles to be excellent drug delivery vehicles, since after loading in the wet state and storage of the loaded particles in the dehydrated state release could possibly be triggered upon re-hydration. Hydrated eADF4(C16) particles show an elastic modulus of 2.99 MPa ± 0.90 MPa, which is three orders of magnitude lower than that of the dried state. Interestingly, the large decrease in modulus after hydration is also observed for the particles' natural prototype, the *Araneus diadematus* dragline fiber.[22]

A fatigue test with 61 compression–decompression repetitions was performed on hydrated eADF4(C16) particles indicating no change in the elastic modulus (Fig. 2e and Fig. 2 ESI†); such a difference to the dehydrated particles indicates a high material elasticity of the hydrated particles with water acting as the plasticizer.

Effect of molecular weight and crosslinking on particle properties

Previously it has been shown that crosslinking of eADF4(C16) proteins has an impact on the mechanical, chemical and proteolytic stability of different morphologies.[3,5,7] Especially for eADF4(C16) hydrogels an impact of chemical crosslinking on the rheological behavior of the hydrogels has been observed.[4]

In order to determine the effect of crosslinking on the mechanical behavior of the particles, the influence of molecular weight (influencing physical crosslinking) (Fig. 3a) and chemical crosslinking (Fig. 3b) was analyzed. First, the elastic modulus of particles made up of eADF4 proteins with identical amino acid composition but different molecular weights of 24.6, 47.7 and 93.8 kDa was investigated. Hydrated eADF4(C8) particles showed an elastic modulus of 2.58 MPa ± 1.09 MPa and eADF4(C32) particles of 5.55 MPa ± 1.48 MPa, being respectively lower and higher than that of eADF4(C16). The

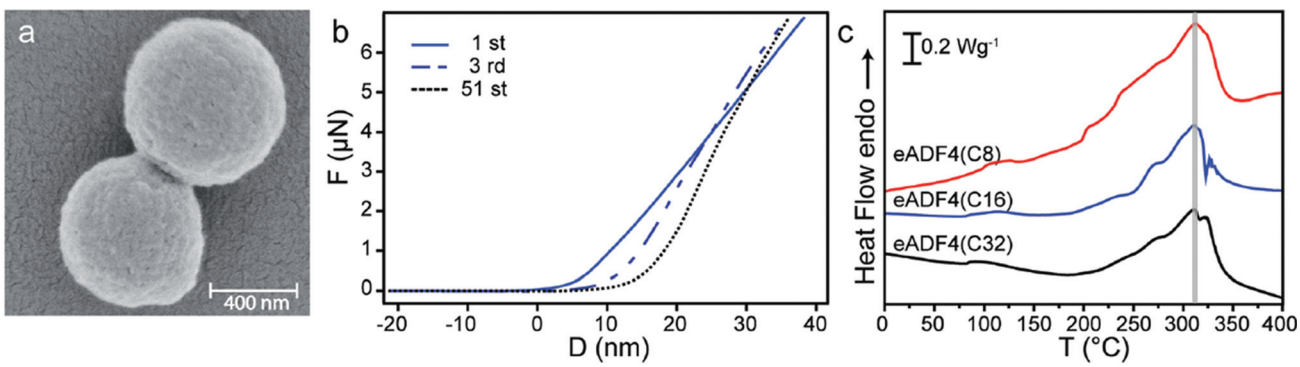

Fig. 1 (a) SEM image of eADF4(C16) particles. (b) Fatigue tests of dry eADF4(C16) particles. Force–distance curves of an individual particle showing an increasing slope and a shift in the contact point with ongoing deformations. (c) Differential scanning calorimetry (DSC) measurements of eADF4 proteins with identical amino acid composition and molecular weights of 24.6 (eADF4(C8)), 47.7 (eADF4(C16)) and 93.8 kDa (eADF4(C32)).

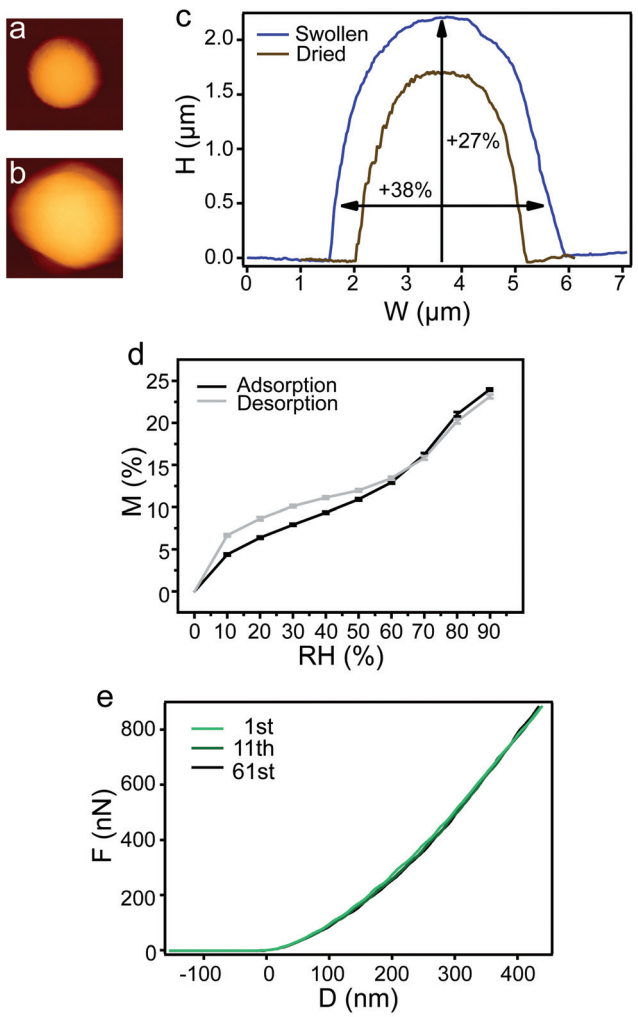

Fig. 2 Swelling of an exemplary eADF4(C16) particle monitored by AFM in the (a) dried and (b) hydrated state. (c) Comparison of the corresponding height profiles. (d) Mass increase and decrease due to water adsorption and desorption of eADF4(C16) particles were identical after 10 repetitions (error bars shown at every 10% RH). (e) Mechanical fatigue test on the eADF4(C16) particle indicating material elasticity.

influence of molecular weight on the mechanical behavior can be explained by higher inter- and intramolecular interactions, leading to a stiffer network for larger proteins.

Next, the impact of chemical crosslinking on the deformation behavior of the eADF4(C16) particles was studied (Fig. 3b). It has already been shown that chemical crosslinking has an influence on the chemical stability of eADF4(C16) particles;[7] therefore an influence on the mechanical behavior was also conceivable. As described previously, there are two different routes of adding the chemical crosslinking molecules, either before (CLpre) or after (CLpost) particle formation (Fig. 3 ESI†), showing a distinct influence on the micromechanical behavior of eADF4(C16) particles (Fig. 3b). The diffusion technique (CLpost) leads to stiffer particles compared to the mixing technique (CLpre). Generally, the increase in modulus with crosslinking is in agreement with earlier experiments on hydrogels.[4,5] However, the relative stiffening effect is not as pronounced. A reason for this observation is attributed to the high β-sheet content (64%), already in the non-crosslinked particles.[2] Consequently, additional covalent bonding has only a moderate influence on mechanical properties. In the case of hydrogels, the amount of β-sheets is lower (around 40%) as well as the modulus (kPa range). There, introduction of covalent bonds leads to a manifold increase in elastic modulus.

Besides the different mechanical properties, chemically crosslinked particles showed also different swelling behavior (Fig. 3c) compared to non-CL particles, since the protein network is more stabilized due to the formation of di-tyrosines. CLpost particles are found to exhibit a more pronounced swelling than CLpre particles. The thermal decomposition temperature, in contrast, was apparently not significantly influenced by chemical crosslinking (Fig. 3d).

The differences both in mechanical and swelling properties of differently crosslinked particles can be attributed to the respective distribution of the gained di-tyrosine crosslinks throughout the particles. In the case of CLpre, the crosslinking is homogeneously distributed throughout the particles resulting in a spatially uniform strengthened protein network (Scheme 1). With the CLpost route, crosslinking occurs mainly at the surface of the particles (Scheme 1), since diffusion into the particle is partially hindered by steric and electrostatic repulsion. Therefore, in the regime which is probed in the force spectroscopy experiments, *i.e.* small deformations of up to 10% of the diameter, CLpost particles exhibit a locally higher crosslinking density (on the surface) compared to the CLpre particles. As a consequence the detected modulus is higher. Analogously, the less crosslinked interior of CLpost particles is more prone to collapsing during dehydration than the homogeneously stabilized network in CLpre. Thus, a more pronounced deswelling/swelling is observed for CLpost particles.

Conclusions

In summary, our data show the extraordinary mechanical stability of eADF4 particles in the dried state. The high modulus and chemical stability allows applications as fillers in composite materials. However, since the particles are subject to considerable swelling in humid environments, this might be a constraint for certain applications. Compared to the dehydrated state, swollen particles are much softer, but still exhibit remarkable mechanics which can be tuned selectively by adjusting the molecular weight of the employed protein or by chemical crosslinking. Mechanical fatigue tests have shown the elasticity of the swollen material in contrast to the situation in the dried state, where a plastic response upon deformation was observed. Hydration and dehydration of eADF4(C16) particles is fully reversible. This is a crucial feature with regard to exploring the particles' potential for drug delivery or for cosmetic applications, while odorants or drugs can be

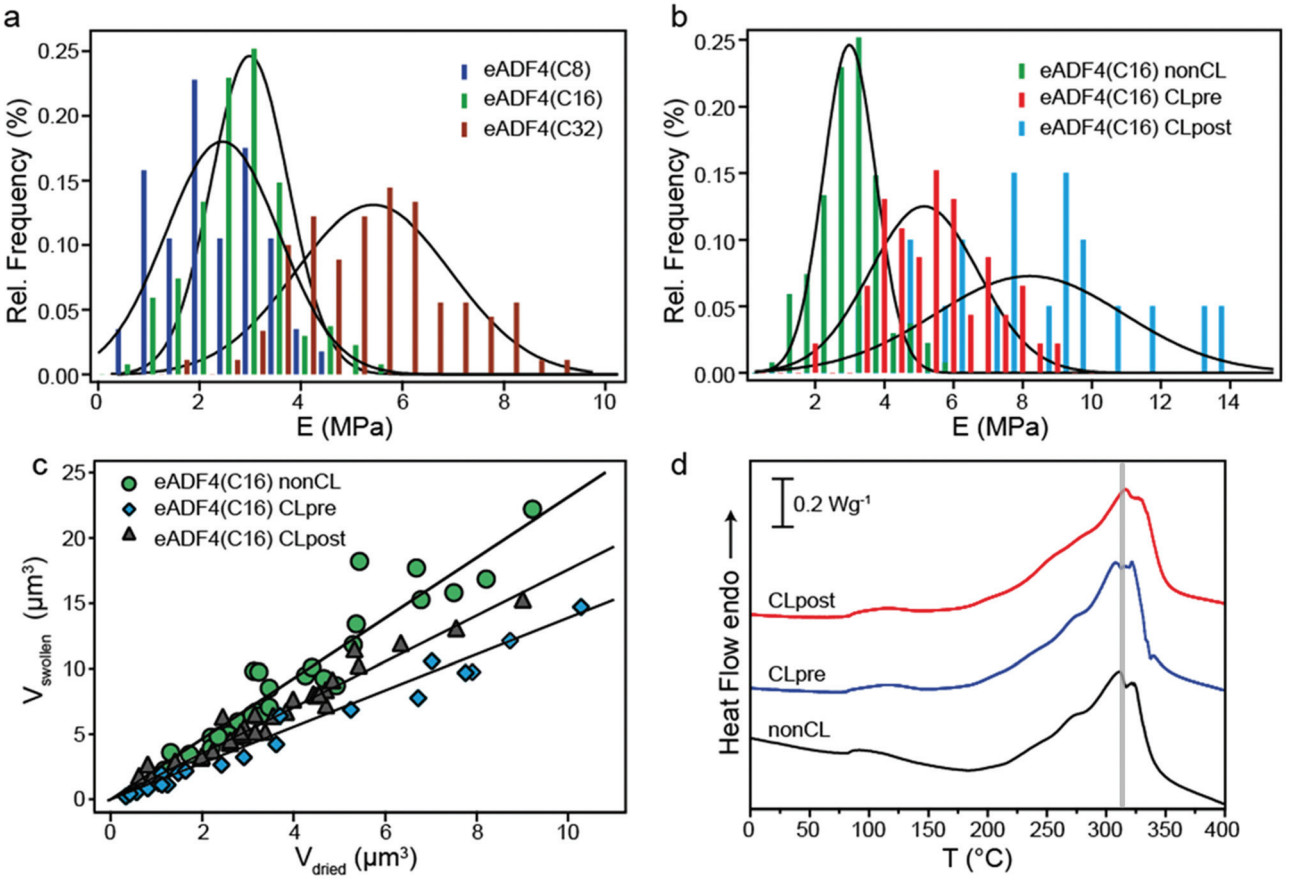

Fig. 3 (a) Histogram showing the distribution of elastic moduli of eADF4(C8), eADF4(C16) and eADF4(C32) spider silk particles in the hydrated state ($n > 50$). The solid lines represent Gaussian fits. (b) Histogram showing the distribution of elastic moduli for hydrated non-crosslinked and chemically crosslinked eADF4(C16) particles with the solid lines representing Gaussian fits of the data. Crosslinking molecules were added before (pre) or after (post) particle formation leading to differently crosslinked particles. (c) Hydrated *vs.* dried volume of chemically crosslinked and non-crosslinked eADF4(C16) particles. CLpre particles show significantly less swelling than all the other particles with a volume swelling factor of 1.40. CLpost particles exhibit a swelling factor of 1.76, which is in between that of non-crosslinked and 'pre' crosslinked particles. Solid lines represent linear fits. (d) DSC scans of dehydrated chemically crosslinked and non-crosslinked eADF4(C16) particles.

loaded by a diffusion controlled process or by co-precipitation.[7] Subsequent drying yields a stable storage form with the encapsulated molecules safely entrapped. In physiological solutions the particles swell again, and diffusion driven release of the encapsulate is enabled. Based on the mechanical data, it is now feasible to unravel novel materials science applications of spider silk particles in further studies.

Materials and methods

Protein production and purification

The recombinant spider silk protein eADF4(C16) (47.7 kDa) consists of 16 repetitions of the C-module mimicking the highly repetitive core sequence of ADF4.[23] eADF4(C8) consists of eight repetitions (24.6 kDa), and eADF4(C32) (93.8 kDa) of 32 repetitions, which results in proteins with half or double the molecular weight of eADF4(C16), respectively. Production and purification of all proteins was carried out as described for eADF4(C16) previously.[23]

Particle formation

The lyophilized proteins were dissolved in GdmSCN (6 M) and dialyzed against tris(hydroxymethyl)–aminomethane–HCl (Tris-buffer) (10 mM) pH 8 overnight at 20 °C. For particle formation, the aqueous protein solution was dialyzed against a tenfold volume of 1 M potassium phosphate, pH 8, for one hour at room temperature (RT).[1,2] After precipitation, the particles were washed three times with Tris-buffer.

Crosslinking

Crosslinking of the proteins was carried out as described previously.[7] Two different routes of crosslinking were tested. CLpre describes a procedure where APS (ammonium persulfate) (10 mM) and Rubpy (tris(2,2′-bipyridyl) dichloro ruthenium(II)) (100 µM) (Sigma-Aldrich, Germany) were mixed with the aqueous protein solution followed by -precipitation. CLpost reflects a technique by which the crosslinking molecules diffused into the pre-formed particles (Fig. 3 ESI†).[24]

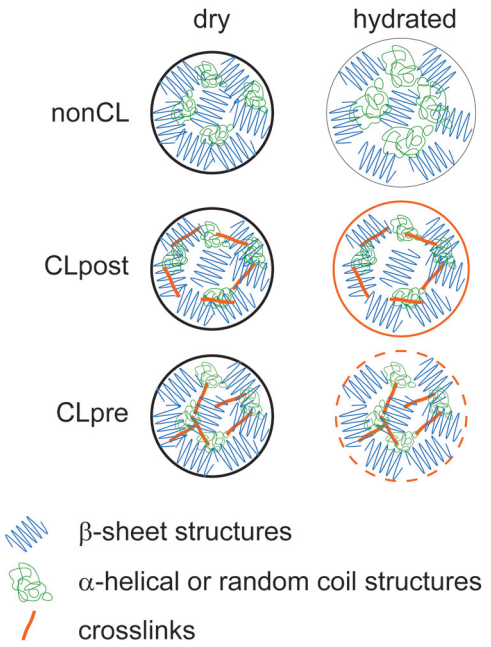

Scheme 1 The swelling as well as the mechanical behavior of eADF4 particles depends on the crosslinking process. Swelling is limited and the elastic modulus is increased by crosslinking. The CLpre route leads to particles with a homogeneous crosslinking and less swelling with a higher elasticity than particles crosslinked by the CLpost route.

Scanning electron microscopy (SEM)

Sample preparation was performed as described previously.[7] SEM images were made with a 1450EsB Cross Beam (Zeiss, Germany) at an accelerating voltage of 3 kV.

Differential scanning calorimetry (DSC)

For DSC scans, protein samples (5–7 mg) were sealed in aluminium pans and heated under constant nitrogen gas flow at 5 °C min^{-1} using an SDTA 821e differential scanning calorimeter (Mettler Toledo, Germany) equipped with a ceramic sensor with a 56-fold Au–Au–Pd thermocouple row. Before starting the experiment, the samples were heated to 110 °C in order to evaporate the remaining water. After an equilibration step (10 min) the samples were cooled to −40 °C, and finally the measurements were started by heating the samples to 400 °C.

Water adsorption and desorption measurements

Measurements were performed using a Moisture Analyzer IGASorp (Hiden Analytical, Germany) with a microbalance resolution of 0.1 μg and a minimal humidity step change of 0.2%. eADF4(C16) particles (*ca.* 20 mg) were incubated at a constant temperature of 25 °C and a nitrogen flow rate of 200 mL min^{-1}, while the relative humidity was increased from 0 to 90%. 10 adsorption and desorption cycles were performed assuming an adsorption of zero at 0% relative humidity.

Sample preparation for AFM

5 μl of an eADF4(C16) particle suspension (*ca.* 5 mg mL^{-1}) were transferred into a poly-ethyleneimine (PEI) coated Petri dish (diameter 2 cm, height 0.5 cm). PEI was used to promote particle adhesion. Non-adhesive particles were rinsed with deionized water (Milli-Q® Academic, Millipore, Billerica, USA). The Petri dish was either filled with deionized water (1.5 mL) or left empty, respectively, before mechanical testing.

Atomic force microscopy (AFM)

All measurements were performed with an AFM NanoWizard® I (JPK Instruments, Berlin, Germany), combined with an inverted optical microscope Axiovert 200 (Carl Zeiss MicroImaging, Jena, Germany) which is equipped with a 20× and a 63× oil immersion objective. All measurements were performed at room temperature.

AFM imaging

All topography images were obtained in intermittent contact mode. For measurements in water, soft cantilevers were chosen (NSC 36 and CSC 17, no Al coating, MikroMasch, Tallinn, Estonia) with a typical spring constant of 0.95 N m^{-1} and 0.15 N m^{-1}, respectively. Imaging in air was done using a stiffer cantilever (NSC 14, no Al coating, MikroMasch) with a typical spring constant of 5 N m^{-1}.

AFM force spectroscopy

For the force spectroscopy experiments modified cantilevers (colloidal probe) were used: instead of a sharp tip a silica bead with a diameter in the range of 20–50 μm (Polysciences Europe GmbH, Eppelheim, Germany) was glued (two-component epoxy glue, UHU Endfest 300, UHU GmbH & Co. KG, Bühl, Germany) under the very front of a tipless cantilever (NSC 12, no Al coating, MikroMasch). Prior to the measurements all used cantilevers were calibrated against the glass substrate in order to obtain their optical lever sensitivity which equals the slope of the approach part of the resulting force–deformation curve. The exact spring constant of each cantilever was obtained before any modification by employing the thermal noise method.[25] The approach and retraction velocity of the cantilever was 5 μm s^{-1} for all measurements, and one cycle was performed in 2 s. For the fatigue experiments a dwell time of 1 s was kept between two consecutive cycles.

Mechanics of elastic compression

One of the fundamental theories describing the mechanics of elastic compression was provided by Hertz.[18] In the case of normal loads for isotropic linear elastic bodies, when adhesion or friction are neglected, the relation between deformation d and applied force F is given according to eqn (1) for a sphere–sphere geometry:

$$F = \frac{4}{3} \times E \times d^{\frac{3}{2}} \times \sqrt{R} \quad (1)$$

Here, E and R are the relative Young's modulus and radius, respectively, given in eqn (2) and (3), with ν being Poisson's ratio (assumed to be 0.5 for spider silk). The indices refer to the two objects approaching, *e.g.*, the colloidal probe and the spherical soft particle. In the case of a non-deformable probe

(*e.g.*, a glass bead) its contribution to the combined elastic modulus is negligible.

$$\frac{1}{E} = \frac{1-\nu_1{}^2}{E_1} + \frac{1-\nu_2{}^2}{E_2} \quad (2)$$

$$\frac{1}{R} = \frac{1}{R_1} + \frac{1}{R_2} \quad (3)$$

Acknowledgements

The authors would like to thank Ute Kuhn for carrying out the DSC measurements and the Lehrstuhl Metallische Werkstoffe (University of Bayreuth) for providing access to the SEM. This work was financially supported by the Bundesministerium für Bildung und Forschung (BMBF, grant number 13N11340) and by the Deutsche Forschungsgemeinschaft (DFG, grant number FE 600/12-1 and SCHE 603/9-1).

Notes and references

1 A. Lammel, M. Schwab, U. Slotta, G. Winter and T. Scheibel, *ChemSusChem*, 2008, **1**, 413–416.
2 U. K. Slotta, S. Rammensee, S. Gorb and T. Scheibel, *Angew. Chem., Int. Ed.*, 2008, **47**, 4592–4594.
3 K. D. Hermanson, D. Huemmerich, T. Scheibel and A. R. Bausch, *Adv. Mater.*, 2007, **19**, 1810–1815.
4 S. Rammensee, D. Huemmerich, K. D. Hermanson, T. Scheibel and A. R. Bausch, *Appl. Phys. A: Mater.*, 2006, **82**, 261–264.
5 K. Schacht and T. Scheibel, *Biomacromolecules*, 2011, **12**, 2488–2495.
6 A. Leal-Egana and T. Scheibel, *J. Mater. Chem.*, 2012, **22**, 14330–14336.
7 C. Blüm and T. R. Scheibel, *BioNanoSci*, 2012, **2**, 67–74.
8 A. Lammel, M. Schwab, M. Hofer, G. Winter and T. Scheibel, *Biomaterials*, 2011, **32**, 2233–2240.
9 M. Hofer, G. Winter and J. Myschik, *Biomaterials*, 2012, **33**, 1554–1562.
10 B. Liebmann, D. Huemmerich, T. Scheibel and M. Fehr, *Colloids Surf., A*, 2008, **331**, 126–132.
11 H. J. Butt, B. Cappella and M. Kappl, *Surf. Sci. Rep.*, 2005, **59**, 1–152.
12 M. E. McConney, S. Singamaneni and V. V. Tsukruk, *Polym. Rev.*, 2010, **50**, 235–286.
13 A. Fery and R. Weinkamer, *Polymer*, 2007, **48**, 7221–7235.
14 J. Erath, S. Schmidt and A. Fery, *Soft Matter*, 2010, **6**, 1432–1437.
15 S. Rentsch, R. Pericet-Camara, G. Papastavrou and M. Borkovec, *Phys. Chem. Chem. Phys.*, 2006, **8**, 2531–2538.
16 Z. Deng, V. Lulevich, F. T. Liu and G. Y. Liu, *J. Phys. Chem. B*, 2010, **114**, 5971–5982.
17 N. Helfricht, M. Klug, A. Mark, V. Kuznetsov, C. Blüm, T. Scheibel and G. Papastavrou, *Biomater. Sci.*, 2013, DOI: 10.1039/c3bm60109a.
18 H. Hertz, *Reine Ang. Math.*, 1881, **92**, 156–171.
19 K. Spiess, R. Ene, C. D. Keenan, J. Senker, F. Kremer and T. Scheibel, *J. Mater. Chem.*, 2011, **21**, 13594–13604.
20 F. Junghans, M. Morawietz, U. Conrad, T. Scheibel, A. Heilmann and U. Spohn, *Appl. Phys. A: Solid Surf.*, 2006, **82**, 253–260.
21 P. J. Flory, *Principles of Polymer Chemistry*, Cornell University Press, Ithaca, 1953.
22 K. Savage and J. Gosline, *J. Exp. Biol.*, 2008, **211**, 1937–1947.
23 D. Huemmerich, C. W. Helsen, S. Quedzuweit, J. Oschmann, R. Rudolph and T. Scheibel, *Biochemistry*, 2004, **43**, 13604–13612.
24 D. A. Fancy and T. Kodadek, *Proc. Natl. Acad. Sci. U. S. A.*, 1999, **96**, 6020–6024.
25 J. L. Hutter and J. Bechhoefer, *Rev. Sci. Instrum.*, 1993, **64**, 1868–1873.